ISSN 2070-2051, Protection of Metals and Physical Chemistry of Surfaces, 2020, Vol. 56, No. 1, pp. 169–179. © Pleiades Publishing, Ltd., 2020.

NEW SUBSTANCES, MATERIALS AND COATINGS

High Temperature Oxidation Resistance of FeCrAlTiY-MCrAlY (M = Co and Ni) Coatings on Carbon Steel Prepared by Flame Spray Technique

Dedi Holden Simbolon[a], Januaris Pane[a], Bambang Hermanto[b], Ahmad Afandi[b], Kerista Sebayang[a], Marhaposan Situmorang[a], and Toto Sudiro[b, *]

[a] *Postgraduate Program of Physics, Faculty of Mathematic and Natural Science, University of Sumatera Utara, Medan, Sumatera Utara, 20155 Indonesia*

[b] *Research Center for Physics, Indonesian Institute of Sciences, Kompleks PUSPIPTEK Serpong, Tangerang Selatan, Banten, 15310 Indonesia*

**e-mail: toto011@lipi.go.id*

Received February 12, 2019; revised May 10, 2019; accepted May 16, 2019

Abstract—Four different composition of FeCrAlTiY-*x* MCrAlY (M = Co and Ni, *x* = 0, 10, 20, and 30 in mass %) coatings were prepared onto carbon steel substrate using a flame spray technique. The high temperature oxidation resistance of the coating and uncoated samples was studied cyclically at 700°C for 8 times. X-ray diffraction (XRD) and scanning electron microscope equipped with energy dispersive X-ray spectrometer (SEM-EDX) were used to investigate the phase composition and morphologies of the coating before and after oxidation. Depending on the coating composition, the coatings are composed of FeCr, $Fe(Cr,Al)_2O_4$, $(Co,Ni)Cr_2O_4$ and FeO. After high temperature oxidation test, it was found that the carbon steel experienced high oxidation rate at the aforesaid temperature, forming a thick Fe-oxides layer. Even if a protective Al_2O_3 or Cr_2O_3 layer is not formed on the coating surface, the flame sprayed FeCrAlTiY–MCrAlY coatings effectively improve the resistance of carbon steel toward oxidation at high temperature due to the formation of Fe_2O_3 and spinel oxides. According to the results, the 30 mass % MCrAlY coating exhibited a lowest mass gain after exposure at 700°C for 8 cycles.

Keywords: FeCrAlTiY, MCrAlY, carbon steel, coating, flame spray, oxidation

DOI: 10.1134/S2070205120010219

1. INTRODUCTION

The mechanical strength and resistance of material toward oxidation and corrosion are important factors in selecting materials for high temperature applications. Carbon steels have been widely used for structural applications because of its lower cost and good mechanical properties. The critical issues for the use of low carbon steel with the increase of operating temperature are oxidation and corrosion resistance. The potential application of this material is restricted when it is exposed to high temperature and oxidizing atmospheres [1–3]. This leads to the thickness loss of the sample due to iron oxidation, forming a thick Fe-oxides layers consisting of Fe_2O_3, Fe_3O_4 and FeO on the steel surface [3–6]. The steels tend to easily oxidize at higher temperatures. Accordingly, surface treatment is required to overcome the aforesaid limitations.

FeCrAlY [7, 8] and MCrAlY (M = Co and/or Ni) [9, 10] either as alloys and coatings have been intensively studied due to their resistance toward oxidant and chemical attack at high temperature and aggressive environments. However, the development of materials for advanced energy applications still encounters some challenges because their structural and high temperature properties such as the formation of a protective oxide layer are often affected by its composition and oxidizing conditions including temperature, time and atmosphere. Modifying the material composition can be considered to enhance its oxidation resistance. Accordingly, it is important to investigate and clarify whether the combination of both materials, FeCrAlTiY and MCrAlY, applied as composite coating can possibly improve the oxidation resistance of the carbon steel at high temperature.

Many studies utilized thermal spray coating techniques such as high velocity oxygen fuel (HVOF) [9, 11, 12], atmospheric plasma spray coating (APS) [13] and flame spray techniques [14–19] to prepare the metallic or nonmetallic coatings for oxidation, corrosion, and wear resistant coating applications. Basically, the feedstocks of powder, rod or wire are heated into a molten or semimolten state and then accelerated toward a substrate surface to form a coating layer [14,

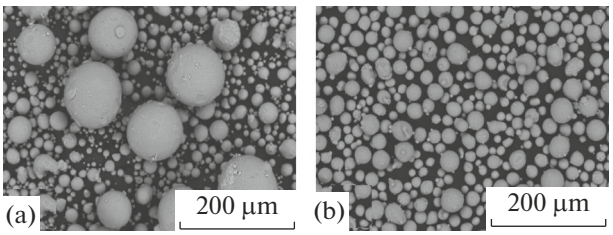

Fig. 1. BSE SEM images of (a) FeCrAlTiY dan (b) MCrAlY powders.

20]. It is noteworthy that the coating preparation using a flame spray method has several advantages, such as easy to use, low cost, lower flame temperatures (prevent thermal decomposition) [19], quiet operation and applicable to spray various materials. A number of studies used this technique to deposit Fluorhydroxyapatite [19], FeCr [14, 15], composite [16], porous hydroxyapatite coatings [17] and Y_2O_3 film [18] on the various substrate materials.

In this study we reported the high temperature oxidation characteristics of FeCrAlTiY coatings containing 0, 10, 20, and 30 mass % MCrAlY. It was expected that the addition of MCrAlY could promote the formation of a protective oxide scale and enhance the resistance of sample against oxidation. The coating was deposited on the surface of low carbon steel using a flame spray technique. Their resistance against oxidation at high temperature was studied at 700°C for 8 cycles and compared to the low carbon steel. X-ray diffraction and SEM-EDX were used to study the phase and microstructure of the coating before and after oxidation.

2. EXPERIMENTAL

2.1 Sample Preparation

In this study, carbon steel namely ST 41 (98.90 Fe, 0.499 Mn, 0.239 Si, 0.0989 C, 0.0419 Cr, 0.0108 Cu, 0.0199 Ni, 0.053 Ta, 0.0174 P, 0.0029 S, 0.0133 Ti, and 0.0435 Al in mass %) with a size of 1 × 1 × 0.3 cm was used as substrate. A small hole with 1 mm in diameter was drilled in the top-middle of the substrate. It was used to hang the sample during coating process. For coating preparation, the surface of the samples was mechanically polished using various grit of abrasive SiC papers ranging in size from #150 to #800 to obtain a flat surface and to remove the scales and contaminants. The samples were then ultrasonically cleaned in ethanol solution for 10 min and dried using hot blowing air. Subsequently, the sample surface was sand blasted using brown fused alumina with a pressure of 12 bar in order to increase the bond strength between coating and substrate. Careful substrate cleaning after sand blasting was carried out to remove the contaminants from the substrate surface.

Table 1. Nominal composition of FeCrAlTiY powder

Element	Cr	Al	Ti	Ni	Mn	Y	Cu	Fe
mass %	17.2	6.6	0.58	0.47	0.36	0.097	0.097	Balance

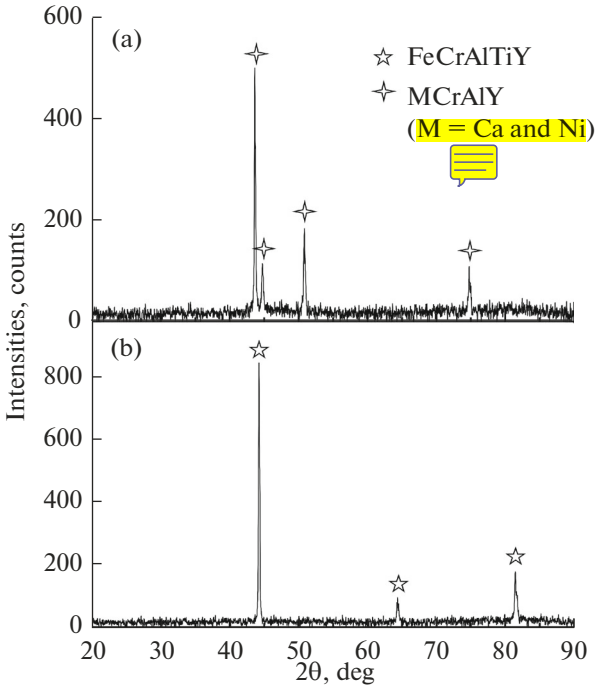

Fig. 2. X-ray diffraction patterns of (a) FeCrAlTiY dan (b) MCrAlY powders.

2.2 Coating Powder and Composition

Two kinds of commercial powders as FeCrAlTiY (Sandvik Materials Technology Ltd) and MCrAlY with M = Co and Ni (Sulzer Metco Co. Ltd) with an average particle size of about 106 and 45 μm, respectively were used as starting material in this study. Both powders have a spherical shape as shown in the BSE SEM images of Fig. 1 and should be able to pass through the flame spray nozzle. The MCrAlY powder might play a role to fill the gaps or pores between the powder of FeCrAlTiY. The nominal composition of FeCrAlTiY and MCrAlY powders is given in Tables 1 and 2, respectively with the powder diffraction patterns presented in Fig. 2.

Four compositions of coating powders as FeCrAlTiY–0, 10, 20 and 30 mass % MCrAlY were prepared. In order to obtain a homogeneous powder mixture, each composition was mixed for 30 min using a rotary milling. The powder was loaded into powder feeder of a flame spraying (Metallisation Flamespray MK74). In this system, acetylene and oxygen gases were used as energy source to produce a flame for heating the feedstock materials and to impact the molten or semi-molten particles on the steel surface. The compressed

air played a role for powder particle carrier/acceleration and spray gun cooling. Moreover, it was used to turn a vibrator assembly to overcome the difficulty of feeding powder. The flame spraying process was performed manually with deposition parameters are presented in Table 3.

2.3 High Temperature Oxidation Test

Before high temperature oxidation test, the samples were put in alumina crucible, weighted using an electronic balance and oxidized in ambient air at 700°C for 8 cycles. The sample was rapidly heated in a muffle furnace at 700°C for 20 h and then cooled for 4 h at room temperature. The aforesaid heating and cooling, namely cyclic oxidation test were repeated for up to 8 times. The mass gain was regularly measured during sample cooling. The oxidation kinetic of sample was evaluated from the difference in mass of the sample after and before oxidation test which is then divided by initial surface area of the sample. The results were plotted in the curve of high temperature oxidation kinetic. In this study, the oxidation resistance of the coatings was compared to the uncoated low carbon steel.

2.4 Characterizations

X-Ray Diffraction (XRD) analysis with CuK_α radiation (λ = 1.541 Å) was used to determine the phase constituent of the coating before and after high temperature cyclic oxidation test. The XRD measurement was conducted using Rigaku Smartlab X-ray diffractometer (40 kV, 30 mA) with the scanning range of 2θ from 20–90 deg, scanning speed of 0.4 and stepping width of 0.01 deg. For the cross-sectional coating analysis, the samples were resin mounted, cross-sectionally cut using abrasive cutting machine, polished using various grit of SiC papers for up to mirror finished and cleaned with flowing water. The composition of the coating was then examined by mean of Hitachi SU3500 Scanning Electron Microscope (SEM) at accelerating voltage of 20 kV equipped with an Energy Dispersive X-Ray Spectrometer (EDX).

3. RESULTS AND DISCUSSION

3.1 Coating Characteristics

3.1.1. Phase Structure. Figure 3 shows the X-ray diffraction patterns of low carbon steel and FeCrAlTiY coatings containing 0, 10, 20 and 30 mass % MCrAlY, respectively prepared by a flame spray technique.

For the comparison, the XRD pattern of the substrate without coating is presented in Fig. 3a. It can be seen that the sharp and narrow peaks of carbon steel substrate consist of three peaks, corresponding to Fe phase. The effect of coating composition on the phase formation of FeCrAlTiY–MCrAlY coatings prepared by a flame spray technique can be explained as follow. For the FeCrAlTiY coating, three phases consisting of FeCr metallic phase and $Fe(Cr,Al)_2O_4$, FeO oxides phases are detected by XRD analysis. Initially, Al_2O_3 and Cr_2O_3 seem to be formed due to Al and Cr affinity for the oxygen. However, they are subsequently solid state reacted with FeO to form $FeAl_2O_4$ [21, 22] and $FeCr_2O_4$ [23, 24]. In this study, it was indicated by the formation of $Fe(Cr,Al)_2O_4$ as detected by XRD analysis. The phase formed in the FeCrAlTiY coatings containing various amount of MCrAlY is almost similar to that of FeCrAlTiY coating without MCrAlY addition. However, the $(Ni,Co)Cr_2O_4$ phase is also identified in

Table 2. Nominal composition of MCrAlY (M=Co and Ni) powder

Element	Co	Ni	Cr	Al	Y
mass %	38.5	32	21	8	0.5

Table 3. Flame spray parameters

Acetylene pressure	0.83 bar
Oxygen pressure	2.07 bar
Compressed air pressure	1.34 bar
Sample to nozzle distance	20 cm

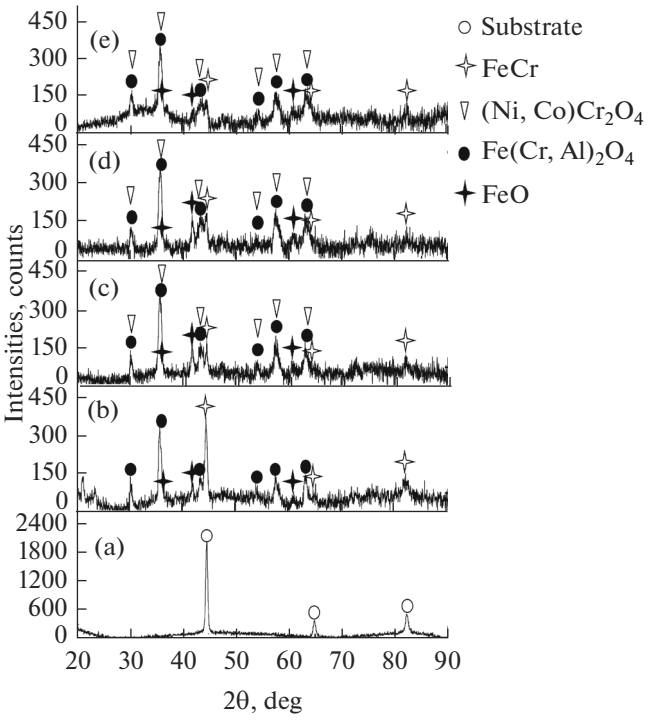

Fig. 3. X-ray diffraction patterns of (a) low carbon steel, FeCrAlTiY coatings with (b) 0, (c) 10, (d) 20 and (e) 30 mass % MCrAlY.

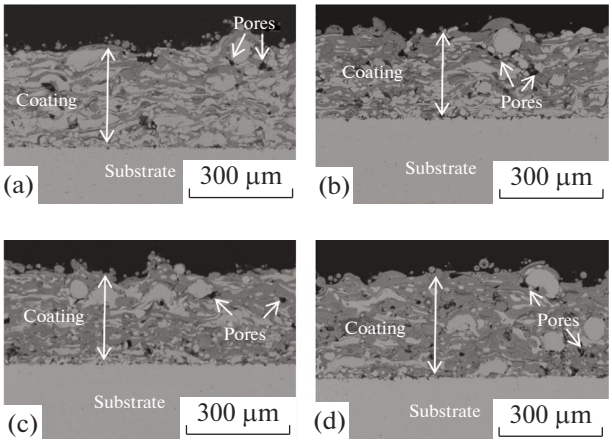

Fig. 4. BSE-SEM cross-sectional microstructures of FeCrAlTiY coatings with (a) 0, (b) 10, (c) 20 and (d) 30 mass % MCrAlY.

the FeCrAlTiY coatings with 10, 20 and 30 mass % MCrAlY. Similarly to $Fe(Cr,Al)_2O_4$, the $(Ni,Co)Cr_2O_4$ spinel structure is formed due to solid state reaction of NiO with Cr_2O_3 and CoO with Cr_2O_3, forming $NiCr_2O_4$ and $CoCr_2O_4$, respectively. Tiantian Zhang et al. (2016) also reported that the spinels can provide the protection against oxidation and corrosion [13].

No phase different is found in the MCrAlY-added coatings. From the results as shown in Fig. 3, the diffraction peak of FeCr phase is likely to decrease and the oxides peaks appear to increase with the addition of MCrAlY. The presence of oxides peaks in all coated samples before high temperature oxidation test indicates that some elements are preferentially oxidized during coating preparation. This is liable to occur due to the use of oxygen and compressed air; and also air atmosphere exposure during coating process at high temperature. M.P. Planche et al. [12] reported that the stoichiometry of the oxygen and fuel mixture affects the combustion temperature. The use of lean combustion ratio results in unconsumable oxygen molecules in the flame. It creates an oxidizing atmosphere. This condition and surrounding air severely enhance the oxidation of molten particles. Thus, the deposited coating becomes oxides-rich [12]. Lowering the diffraction peak intensity of FeCr phase with the addition of MCrAlY reveals that the fraction of FeCr phase in the outer coating layer decreases with the increase of MCrAlY concentration. In addition, the presence of $(Ni,Co)Cr_2O_4$ suggests that some amount of MCrAlY powder is likely to oxidize, even if Co and Ni have lower affinity for the oxygen compared to that of Al and Cr (see Ellingham diagram [25]). In this case, the different in powder size seems to also affect the oxidation of coating powder during coating process. The oxidation of smaller powder is favorable to occur because the smaller particle sizes create larger interfacial areas and increase the number of atoms at the particle interfaces [26]. This results in increasing the oxidation rate of coating powder with the decrease of particle size [27]. The oxygen content in the coatings was affected by in-flight oxidation when the small particles are used and post-impact oxidation when the large particles are used [11]. As mentioned in the experiment, the powder size of MCrAlY is smaller than FeCrAlTiY. Accordingly, MCrAlY powders are likely to oxidize mainly to form $(Ni,Co)Cr_2O_4$. Moreover, some Al from MCrAlY may be oxidized to form Al_2O_3. It undergoes solid state reaction with FeO to form spinel as explained before. While, the oxidation of FeCrAlTiY powders mostly form $Fe(Cr,Al)_2O_4$ and FeO as confirmed by XRD analysis. The formation of aforesaid oxidation products appears covering the FeCr phase. As a result, the diffraction peaks of FeCr phase tend to weak with the increase of MCrAlY concentration.

3.1.2. Microstructure. Figure 4 shows the BSE-SEM cross-sectional images of FeCrAlTiY coatings with different composition of MCrAlY as 0, 10, 20, and 30 mass %.

The cross-sectional images of the samples clearly confirm that the coatings were successfully deposited on the surface of carbon steel using a flame spray technique. It can be seen that the coating and substrate interface is clearly defined. The FeCrAlTiY–MCrAlY coatings show a lamellar structure and well adhere to the substrate with a thickness range of approximately 260–320 μm. The coatings also contain pores and unmelted or partially melted particles. The presence of pores could be due to the existence of various sizes of unmelted particles which can create porosity in the coatings [14, 20] and act as a source for cracks formation [15]. The pores in the coating layer and interconnected pores at the coating interface can act as short circuit path for cations and/or anions diffusion, reducing protection toward corrosion as well as oxidation. Meanwhile, the difference in coating thickness between each composition as shown in Fig. 4 could be related to the thermal spray process which was operated manually.

According to BSE microstructure images of Fig. 4, mostly, the FeCrAlTiY coatings with different content of MCrAlY consist mainly of three distinguished areas: bright, greyish and darkish areas. In order to further determine the composition of corresponding areas, an EDX elemental point analysis was performed. Figure 5 shows the results of EDX spectrum and point analysis in the corresponding area of FeCrAlTiY coatings with 0 and 30 mass % MCrAlY. In the FeCrAlTiY coating (see Fig. 5a), the bright area (Point 1) is mainly composed of 67.06 at % Fe, 15.83 at % Cr and 12.84 at % Al with a very small concentration of Ti and O, which is suspected to be FeCr phase as detected by X-ray diffraction. The greyish area (Points 2 and 3) and darkish area (Points 4) contains mainly of Fe, Cr, Al and O with varying at % con-

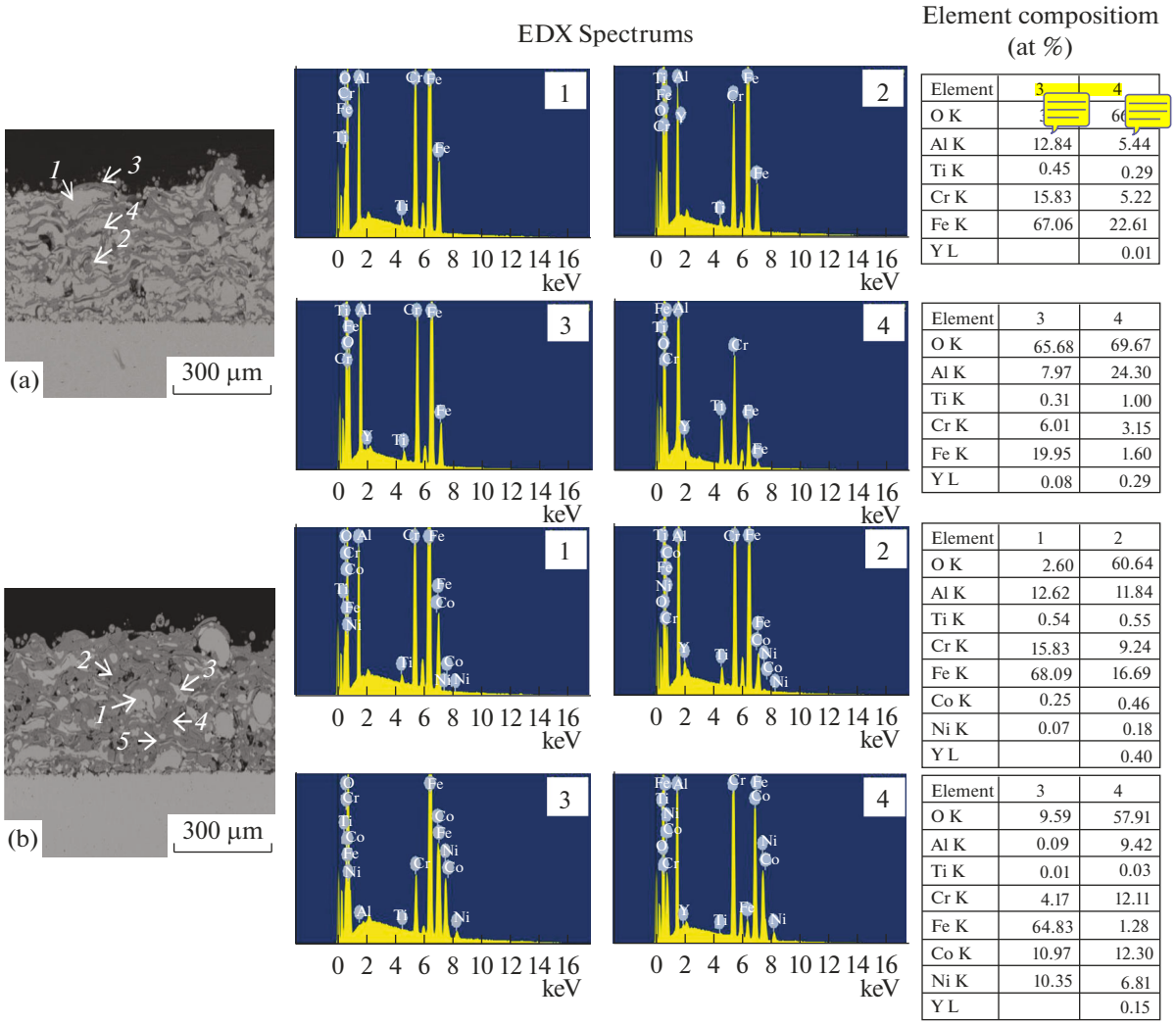

Element	3	4
O K		60
Al K	12.84	5.44
Ti K	0.45	0.29
Cr K	15.83	5.22
Fe K	67.06	22.61
Y L		0.01

Element	3	4
O K	65.68	69.67
Al K	7.97	24.30
Ti K	0.31	1.00
Cr K	6.01	3.15
Fe K	19.95	1.60
Y L	0.08	0.29

Element	1	2
O K	2.60	60.64
Al K	12.62	11.84
Ti K	0.54	0.55
Cr K	15.83	9.24
Fe K	68.09	16.69
Co K	0.25	0.46
Ni K	0.07	0.18
Y L		0.40

Element	3	4
O K	9.59	57.91
Al K	0.09	9.42
Ti K	0.01	0.03
Cr K	4.17	12.11
Fe K	64.83	1.28
Co K	10.97	12.30
Ni K	10.35	6.81
Y L		0.15

Fig. 5. BSE-SEM cross-sectional microstructures and corresponding EDX point analysis in the FeCrAlTiY coatings with (a) 0 and (b) 30 mass % MCrAlY.

tent. In the greyish area, the Fe and O concentrations are higher than Cr and Al, composed of $Fe(Cr,Al)_2O_4$ and FeO phases as detected by XRD analysis. Meanwhile, in the darkish area is rich in Al and O compared to Fe and Cr, namely Al-rich oxide.

On the other hand, for FeCrAlTiY coating with the addition of 30 mass % MCrAlY (see Fig. 5b), two bright areas with different atomic compositions are found. In point 1, the area contains mainly of 68.09 at % Fe, 15.83 at % Cr and 12.62 at % Al with very small content Ti, Co, Ni and O, suggesting that this area is probably FeCr phase as in the FeCrAlTiY coating without MCrAlY addition. Meanwhile in Point 3, the area is composed of 64.83 at % Fe, 10.97 at % Co, 10.35 at % Ni, and 4.17 at % Cr with some amount of oxygen, confirming that the FeCrAlTiY and MCrAlY powders were already reacted during the deposition process. The difference in element concentration of grey area in Points 2 and 4 are also found. EDX point analysis in Point 2 comprises that the area is mainly composed of 16.69 at % Fe, 9.24 at % Cr, 11.84 at % Al and 60.64 at % O with minor elements of Ti, Co, Ni and Y that is suspected to be $Fe(Cr,Al)_2O_4$ phase. Point 4 shows mainly 12.30 at % Co, 6.81 at % Ni, 12.11 at % Cr, 9.42 at % Al and 57.91 at % O with small content of Fe, Ti and Y that this area is probably $(Ni,Co)Cr_2O_4$ phase. The dark area (Point 5) is almost similar to that of in FeCrAlTiY coating which is composed of Al-rich oxide (mainly 23.60 at % Al, 6.70 at % Cr, 5.38 at % Fe, 62.53 at % O and minor element of Ti, Co, Ni and Y). It is formed due to oxidation of Al and other elements from FeCrAlTiY and MCrAlY powders of the coating. However, the fraction of this area is smaller compared to the other areas, similarly to that of in the FeCrAlTiY coating. Thus, it may be not detected by XRD analysis as shown in Fig. 3.

The results of SEM-EDX analysis as presented above are in good agreement with the results of X-ray

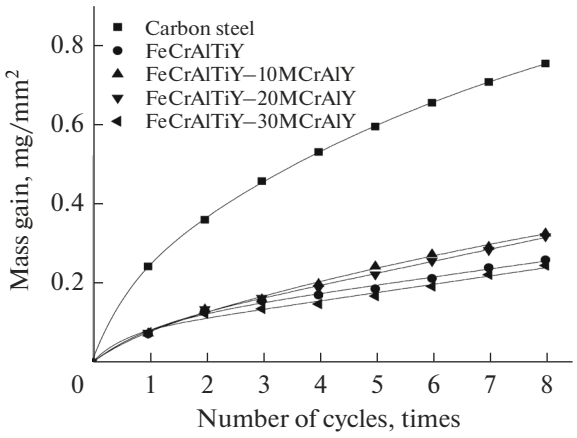

Fig. 6. Mass gain curves of low carbon steel and FeCrAlTiY coatings with 0, 10, 20, 30 mass % MCrAlY after oxidation in air at 700°C for 8 cycles.

diffraction analysis in Fig. 3. Evidently, some coating elements of FeCrAlTiY and MCrAlY such as aluminum and chromium which play a significant role in promoting the formation of a protective Al_2O_3 or Cr_2O_3 scales were preferentially oxidized during coating process. As the MCrAlY content increases, the formation of spinel oxide seems to be increased. For oxidation resistance applications, the formation of oxide during coating process is not expected. This is because the coating becomes depleted with some elements which play a role in promoting the formation of a protective oxide scale and in maintaining the oxide scale protectiveness for long term durability. However, several studies also reported that the spinel oxide can also serves a protection against oxidation and corrosion [13, 22, 23, 28] because the oxygen diffusivity in the spinel oxide is very small [29]. The spinel formation can reduce not only O ions diffusion but also Fe ions and electron free diffusing activities, resulting in high oxidation resistance [23]. Therefore, the formation of spinel oxide in the coating before oxidation at the present study may give a potential beneficial effect as barrier for cation outward diffusion and anion inward diffusion. It may inhibit the growth rate of the oxide scale and improve coating oxidation resistance.

3.2 Coating Characteristics after Exposure at 700°C for 8 Cycles

3.2.1. Oxidation Kinetic. The mass gain curves of carbon steel and FeCrAlTiY coatings containing varying amount of MCrAlY after exposure in air at 700°C as a function of cyclic oxidation time are shown in Fig. 6.

The results show that the mass gain of all samples increases with the increase of cyclic oxidation time, attributed to the formation of oxide scale during sample oxidation. According to the oxidation kinetic curve, the uncoated sample shows the highest mass gain (reached 0.757 mg/mm^2) after 8 cycles of exposure compared to the coated samples from the initial stage of oxidation. This suggests that the uncoated sample has a lowest oxidation resistance. The direct contact of substrate surface to air atmosphere at 700°C leads to the fact that the uncoated sample can be oxidized easily to form oxide layer on the surface of the sample. The scale growth is then controlled by diffusion process of cations and oxygen.

In contrast, the decreasing mass gain of coated sample after oxidation suggests that the FeCrAlTiY–MCrAlY coatings on the surface of carbon steel effectively improve the substrate oxidation resistance. But, their oxidation resistance is compositional dependence. The mass gain curves of Fig. 6 reveal that the total mass gain of FeCrAlTiY coatings containing 0, 10, 20 and 30 mass % MCrAlY after oxidation at 700°C for 8 cycles was 0.261 mg/mm^2, 0.328 mg/mm^2, 0.320 mg/mm^2 and 0.247 mg/mm^2, respectively. All samples show a quick increase in mass gain in the initial stage of oxidation and then a slow increase in mass gain after 1 cyclic time exposure. The high oxidation rate in the initial oxidation period is due to oxide nucleation and rapid oxide formation, and lower oxidation rate after aforesaid condition is due to oxide scale layer turning into growing stage [2, 22]. Since the oxidation curve follows a parabolic rate low, the oxidation kinetic of coated sample is governed by cation and/or anion diffusion similar to that of metals and alloys [29–31]. No significance difference in mass gain is found in the FeCrAlTiY coatings with 10 and 20 mass % MCrAlY content. The mass gain of both samples is higher compared to the MCrAlY-free coating. While, the FeCrAlTiY-30 mass % MCrAlY coating exhibits lowest oxidation rate, resulting best oxidation resistance.

3.2.2. Phase Structure. The X-ray diffraction patterns of uncoated carbon steel substrate and FeCrAlTiY-MCrAlY coatings after high temperature oxidation test at 700°C in air for 8 cycles are presented in Fig. 7.

The results show that the main phase formed as detected by X-ray diffraction measurement on the carbon steel and FeCrAlTiY coating after exposure at 700°C for 8 cycles is Fe_2O_3 phase. As shown in Figs. 7a, 7b, however, the intensity distribution of Fe_2O_3 reflection in both samples is somehow different, once the highest intensity of Fe_2O_3 peak at the diffraction angle of about 64.27 deg and the others at 35.59 deg. This different could be due to a preferred growth orientation of Fe_2O_3 in the uncoated sample and FeCrAlTiY coating during the high temperature oxidation test.

The FeCrAlTiY coatings with 10, 20 and 30 mass % MCrAlY after oxidation at 700°C for 8 cycles display similar peak reflection with intensity different. Based on the analysis results, the predominant phase of FeCrAlTiY coatings with different content of MCrAlY detected by X-ray diffraction is the Fe_2O_3 and

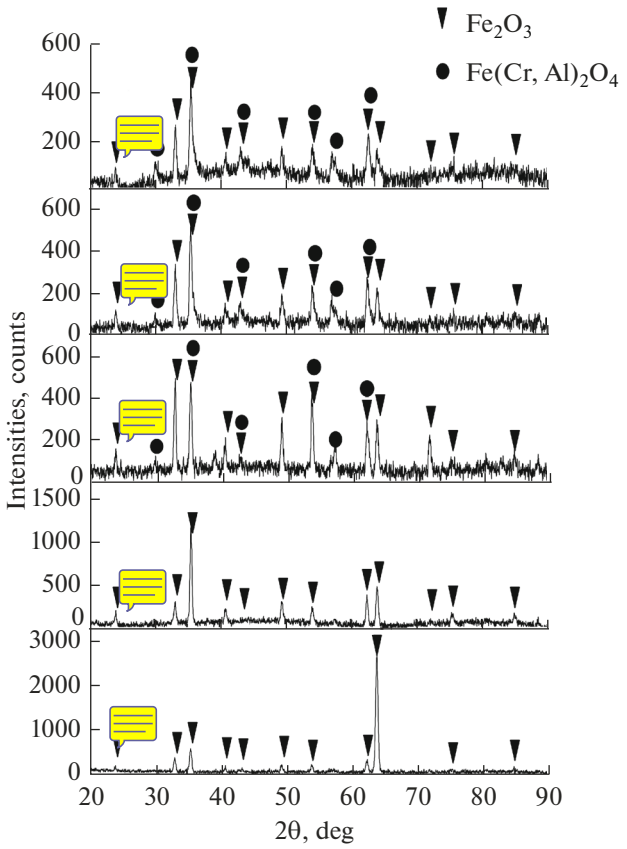

Fig. 7. X-ray diffraction patterns of (a) low carbon steel, FeCrAlTiY coatings with (b) 0, (c) 10, (d) 20 and (e) 30 mass % MCrAlY after oxidation in air at 700°C for 8 cycles.

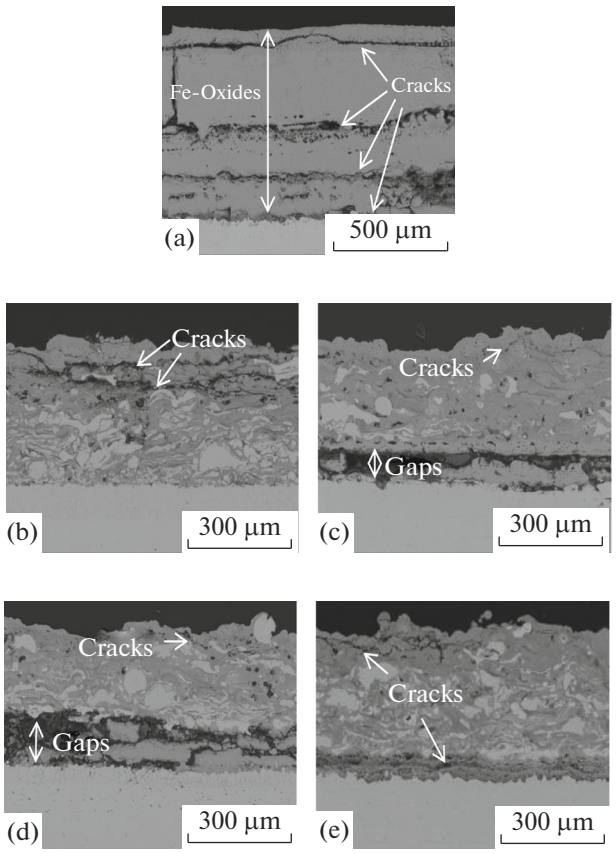

Fig. 8. BSE-SEM cross-sectional microstructures of (a) low carbon steel, FeCrAlTiY coatings with (b) 0, (c) 10, (d) 20 and (e) 30 mass % MCrAlY after oxidation in air at 700°C for 8 cycles.

$Fe(Cr,Al)_2O_4$ phases. It can be seen at diffraction angle of around 33 deg of Fig. 7c,d,e, the intensity of Fe_2O_3 peak tends to decrease with the increase of MCrAlY content. This suggests that the growth of Fe_2O_3 scale decreases as MCrAlY content increases. It seems that the presence of spinel oxide before oxidation affects the formation and growth of Fe_2O_3 scale, decreasing Fe outward diffusion and oxygen inward diffusion. In addition, it is important to note that the Al_2O_3 or Cr_2O_3 scale is not detected by X-ray diffraction in the FeCrAlTiY–MCrAlY coatings. Mostly Al and Cr elements are already oxidized during coating process as explained earlier.

3.2.3. Coating Microstrusture. Figure 8 shows the microstructural evolution of carbon steel and FeCrAlTiY coatings with 0, 10, 20 and 30 mass % MCrAlY after exposure at 700°C for 8 cycles in air.

It can be seen in Fig. 8a that the uncoated sample forms a thick Fe-oxides scale after oxidation at 700°C for 8 cycles, suggesting the carbon steel suffered from high oxidation rate. According to the results of EDX point analysis as shown in Fig. 9, the external oxide layer with the thickness of about 70 μm is composed by 37.21 at % Fe and 62.79 at % O. This is closed to the atomic ratio of Fe_2O_3 as detected by X-ray diffraction (see Fig. 7a). Beneath the Fe_2O_3 scale, the EDX point analysis of Points 2, 3 and 4 as shown in Fig. 9 indicate that the Fe concentration is lower than O. It is near to the atomic ratio of Fe_3O_4. Accordingly, the oxide scale formed on the carbon steel after exposure at 700°C for 8 cycles is comprised mainly of Fe_2O_3 and Fe_3O_4. In general, the iron oxidation forms triple oxide layers consisting of Fe_2O_3 in the external layer, Fe_3O_4 beneath the Fe_2O_3 scale and FeO scale on the steel surface [3, 4, 6]. The absence of FeO on the substrate surface indicates that the oxygen potential along substrate/oxide interface is comparatively high [5]. In addition, the cracks are found in the Fe_2O_3–Fe_3O_4 scale interface, in the Fe_3O_4 scale and at the oxide/steel interface. Previous study reported that the grain boundaries, cracks and pores play a significant role as the transport path for cations and anions diffusion. The outward iron diffusion and inward oxygen diffusion mainly affected the growth of outer and inner oxide layer, respectively [32].

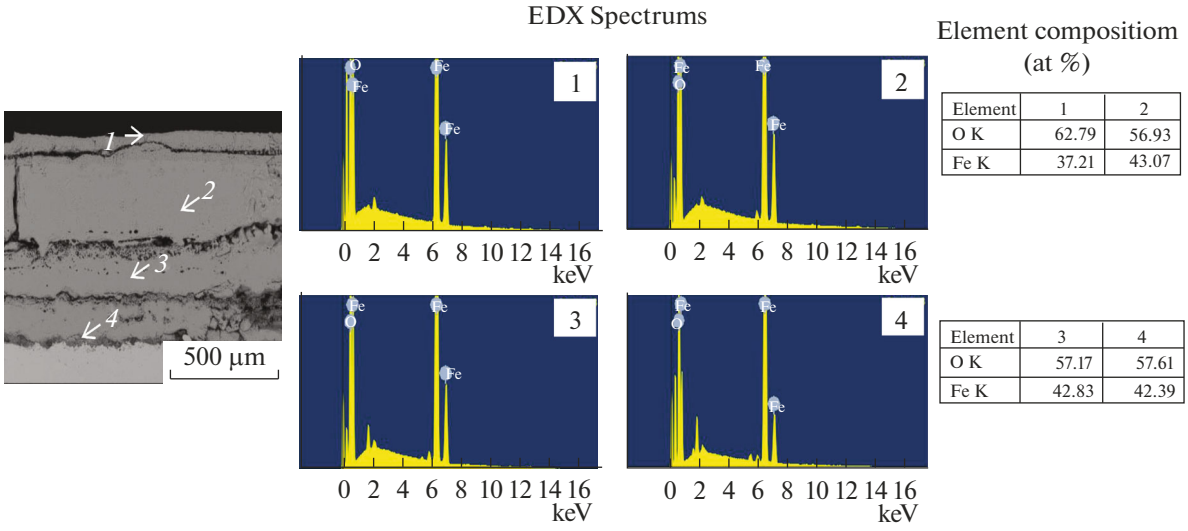

Fig. 9. BSE-SEM cross-sectional microstructures and corresponding EDX point analysis in the carbon steel substrate after oxidation in air at 700°C for 8 cycles.

For the FeCrAlTiY coatings with varying concentration of MCrAlY (0, 10, 20 and 30 mass %), the MCrAlY-free coating exhibits better coating adherence compared to the other composition, but cracks are mostly formed on the coating surface (oxide layer) as in the FeCrAlTiY coatings with 10, 20 and 30 mass % MCrAlY addition. But, the results show that the cracks in the surface of MCrAlY-free coating are much severe than MCrAlY-containing coatings. On the other hand, it is obvious from Fig. 8 that the FeCrAlTiY coatings with 10 and 20 mass % MCrAlY content are spalling from the surface of low carbon steel, leading to oxidation of low carbon steel and the increase of mass gain of the coated samples (see Fig. 6). Unlike the aforesaid results, the 30 mass % MCrAlY coating exhibits much better coating adherence. Accordingly, the mass gain of the FeCrAlTiY and 30 mass % MCrAlY coatings was governed mostly by cations and anions diffusion in the coating, resulting the lower mass gain compared to the 10 and 20 mass % MCrAlY coatings. The adhesion of the coating and substrate is essential for improving the oxidation resistance of carbon steel and for providing long term durability.

According to the results of EDX elemental analysis as presented in Fig. 10a, the oxide layer of FeCrAlTiY coating (Point 1) is composed mainly by 33.59 at % Fe and 66.26 at % O with a very small concentration of Al and Cr which is confirmed by XRD analysis as Fe_2O_3. In the points 2 and 3, the areas are mainly composed of 20.44 at % Fe, 7.15 at % Cr, 8.93 at % Al, 63.03 at % O and 15.95 at % Fe, 10.07 at % Cr, 10.61 at % Al, 62.28 at % O with a small content of Ti and Y, respectively. This is suspected to be $Fe(Cr,Al)_2O_4$ as detected by X-ray diffraction analysis. On the contrary, the darker area of Point 4 is rich in Al and O with small amount of Ti, Cr, Fe and Y. This area is almost similar to that of before oxidation.

Meanwhile, for the FeCrAlTiY-30 mass % MCrAlY coating, the external oxide layer is composed mainly of 32.18 at % Fe and 66.94 at % O similar to that of MCrAlY-free coating which forms Fe_2O_3 scale after exposure for 8 cycles. The grey areas (Points 2 and 4) are composed of two difference compositions. In point 2, it consists of 9.59 at % Fe, 12.49 at % Cr, 13.53 at % Al and 62.62 at % O with a very small concentration of Co, Ni, Ti and Y. Whereas, the area of point 4 contains 22.41 at % Fe, 6.57 at % Cr, 7.33 at % Al, 9.53 at % Co, 7.04 at % Ni and 47.06 at % O with a minor concentration of Ti and Y. Both areas are suspected to be $Fe(Cr,Al)_2O_4$ and $(Co,Ni)Cr_2O_4$, respectively. Point 3 is composed mainly by 81.99 at % Fe, 7.37 at % Co and 3.05 at % Ni with some amount of 0.02 at % Al, 0.24 at % Cr and 7.33 at % O. Al-rich oxide in point 5 consists of 20.55 at % Al, 62.04 at % O, 6.10 at % Fe, 9.70 at % Cr with a small concentration of Ti, Co, Ni and Y.

Based on the results as presented above, it can be summarized that the FeCrAlTiY–MCrAlY coatings did not form a protective Al_2O_3 or Cr_2O_3 scales on its surface. This is attributed to that the Al or Cr elements in the powders were mostly oxidized during coating process to form spinel oxides. Consequently, the coatings become depleted in Al and Cr. The insufficient amount of those elements inhibits the protective oxide formation. Additionally, it is interesting to note that Fe_2O_3 scale is formed in the outer layer of FeCrAlTiY coatings containing varying amount of MCrAlY. The presence of spinel oxide before oxidation and the formation Fe_2O_3 scale after exposure at 700°C for 8 cycles strongly suggest that the aforesaid evidence allows the

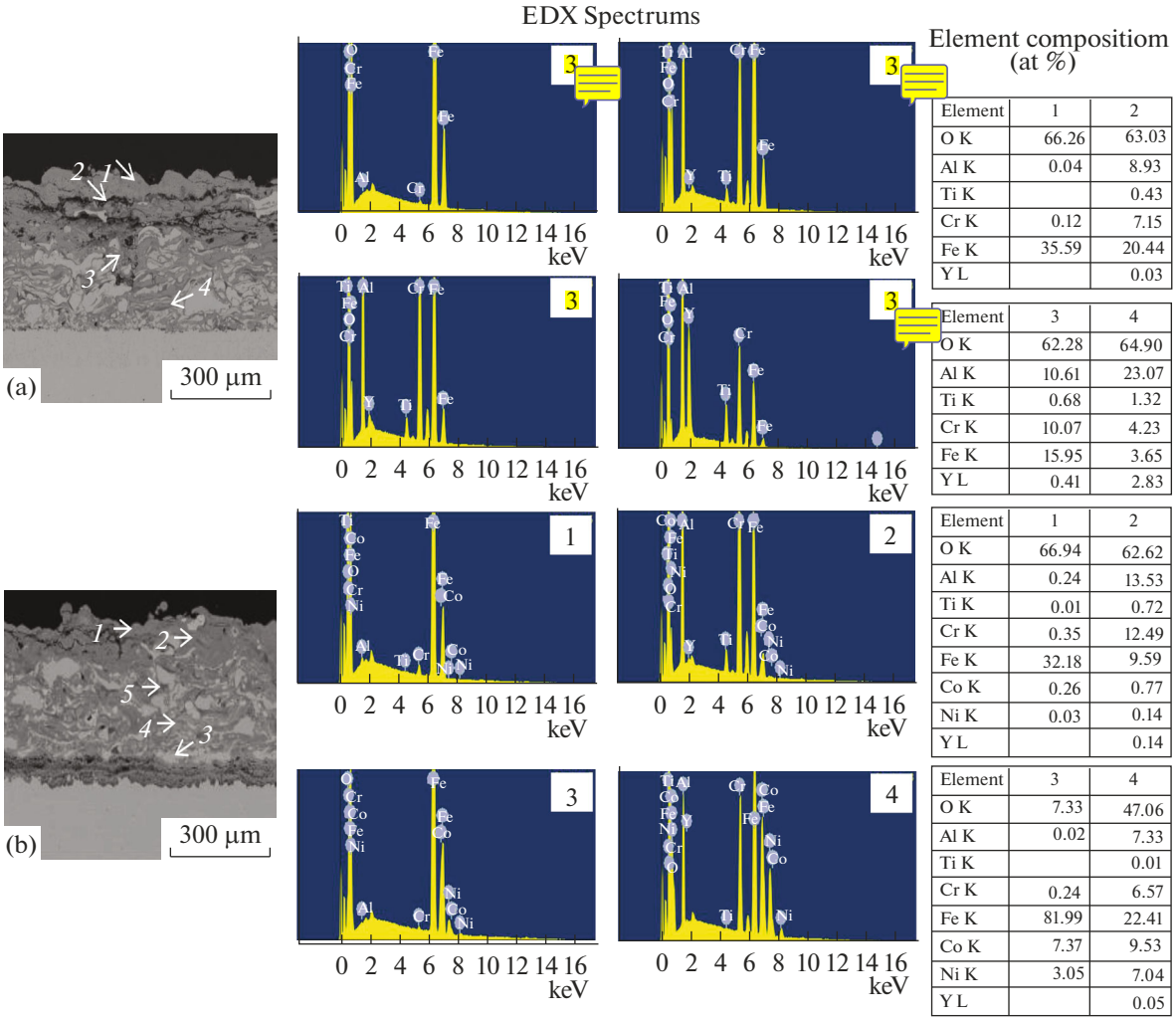

Element	1	2
O K	66.26	63.03
Al K	0.04	8.93
Ti K		0.43
Cr K	0.12	7.15
Fe K	35.59	20.44
Y L		0.03

Element	3	4
O K	62.28	64.90
Al K	10.61	23.07
Ti K	0.68	1.32
Cr K	10.07	4.23
Fe K	15.95	3.65
Y L	0.41	2.83

Element	1	2
O K	66.94	62.62
Al K	0.24	13.53
Ti K	0.01	0.72
Cr K	0.35	12.49
Fe K	32.18	9.59
Co K	0.26	0.77
Ni K	0.03	0.14
Y L		0.14

Element	3	4
O K	7.33	47.06
Al K	0.02	7.33
Ti K		0.01
Cr K	0.24	6.57
Fe K	81.99	22.41
Co K	7.37	9.53
Ni K	3.05	7.04
Y L		0.05

Fig. 10. BSE-SEM cross-sectional microstructures and corresponding EDX point analysis in the FeCrAlTiY coatings with (a) 0 and (b) 30 mass % MCrAlY after oxidation in air at 700°C for 8 cycles.

Fe ions to diffuse outwardly through spinel or defect in the coating and oxidize in the outer layer, forming Fe_2O_3 scale. D. Lussana et al. [33] also reported that during scales growth, the spinel type oxide becomes progressively richer in iron, up to the transformation in hematite (Fe_2O_3). However, the decrease in peak intensity of Fe_2O_3 at around 33 deg of Fig. 7c,d,e reveals that the Fe outward diffusion is likely to decrease with the increase of MCrAlY content. Accordingly, it is important to note that the protection of FeCrAlTiY–MCrAlY coatings prepared by a flame spray technique against cyclic oxidation at high temperature is provided by Fe_2O_3 and spinels formation.

Meanwhile, there are several factors that contribute to the scale cracking and coating adherence or spallation in this study: pore existence [15], growth stress of oxide layer and thermal stress [2, 3, 5, 6, 13, 32, 34, 35] during cyclic oxidation test. As shown in the results of coating microstructure before oxidation, the coating is composed of metallic and oxide phases and also contains some pores. The existence of pores in the coating layer can create or generate the cracks. This results in the decrease of coating adherence. Moreover, the pores at the coating interface tend to become transport path for oxidant and corrodents, reducing its oxidation and corrosion resistance. Under thermal cyclic condition, high thermal stress was generated during high heating and cooling in the coating (between oxide phase and metallic phase) and at the coating/substrate interface due to the difference in thermal expansion coefficient [3, 6, 11, 35]. This turns into oxide cracking mostly in the external oxide layer of FeCrAlTiY–MCrAlY coatings, at the coating interface in 30 mass% MCrAlY coating and coating spallation in the 10 and 20 mass % MCrAlY coatings. In addition, the growth stress of oxide layers enhanced the cracks initiation and propagation. The presence of

cracks in the coating and coating/substrate interface can act as transport parts for oxygen inward diffusion and/or cation outward diffusion. This can accelerate the degradation of coating and substrate. However, the reason for why the FeCrAlTiY coatings with 10 and 20 mass % MCrAlY spalled out from the coating surface and 30 mass % MCrAlY coating more resists to coating exfoliation still need to be understood. The results as presented above show that the FeCrAlTiY-30 mass % MCrAlY coating after exposure at 700°C for 8 cycles exhibits the lowest mass gain associated with best oxidation resistance.

4. CONCLUSIONS

FeCrAlTiY coatings containing various amounts of MCrAlY as 0, 10, 20, 30% by mass were prepared by a flame spray technique on the surface of low carbon steel. The resistance of coated and uncoated samples against oxidation at 700°C for 8 times was investigated. Based on the results obtained the following conclusion can be drawn:

1. Some elements of FeCrAlTiY–MCrAlY coatings were already oxidized during flame sprayed deposition, forming oxide scales of $Fe(Cr,Al)_2O_4$, $(Co,Ni)Cr_2O_4$ and FeO.

2. Carbon steel experienced a high oxidation rate after exposure at 700°C for 8 cycles, forming Fe_2O_3 and Fe_3O_4 scales on its surface.

3. On the contrary, even if a protective Al_2O_3 or Cr_2O_3 scales is not formed after 8 times exposure, the FeCrAlTiY–MCrAlY coatings effectively improve the oxidation resistance of carbon steel due to the formation of spinel oxides and Fe_2O_3 scale.

4. The FeCrAlTiY coating with 30 mass % MCrAlY exhibits lowest mass gain among other composition associated with an excellent oxidation resistance.

FUNDING

This work was financially supported by Program Unggulan 2018 of Indonesian Institute of Sciences. Characterization facilities provided by Research Center for Physics, Indonesian Institute of Sciences were gratefully acknowledged. The authors are grateful to Mr. Ciswandi and Mr. Edi sutiawan for technical support and fruitful discussion.

REFERENCES

1. Canakci, A., Erdemir, F., Varol, T., and Ozkaya, S., *Powder Technol.,* 2013, vol. 247, p. 24.
2. Wang, B., Wu, J., Zhang, Y., Wu, Z., Li, Y., and Xue, W., *Surf. Coat. Technol.,* 2015, vol. 269, p. 302.
3. Sudiro, T., Hia, A.I.J., Ciswandi, Aryanto, D., Hermanto, B., Wismogroho, A.S., and Sebayang, P., *J. Alloys Compd.,* 2018, vol. 732, p. 655.
4. Yu, X., Jiang, Z., Zhao, J., Wei, D., Zhou, C., and Huang, Q., *ISIJ Int.,* 2015, vol. 55, p. 278.
5. Lee, D.-H., Lee, D.-B., and Jung, W.-S., *J. Ceram. Process. Res.,* 2006, vol. 7, p.140.
6. Pinder, L.W., Dawson, K., Tatlock, G.J., and Mahi, F.T., in *Reference Module in Materials Science and Materials Engineering,* Amsterdam: Elsevier, 2017, p. 1.
7. Bennett, M.J. and Bull, S.J., *Mater. Corros.,* 1997, vol. 48, p. 48.
8. Wessel, E., Kochubey, V., Naumenko, D., Niewolak, L., Singheiser, L., and Quadakkers, W.J., *Scr. Mater.,* 2004, vol. 51, p. 987.
9. Feizabadi, A., Doolabi, M.S., Sadrnezhaad, S.K., and Rezaei, M., *J. Alloys Compd.,* 2018, vol. 746, p. 509.
10. Cao, S., Ren, S., Zhou, J., Yu, Y., Wang, L., Guo, C., and Xin, B., *J. Alloys Compd.,* 2018, p. 740.
11. Li, C.-J. and Li, W.-Y., *Surf. Coat. Technol.,* 2002, vol. 162, p. 31.
12. Planche, M.P., Normand, B., Liao, H., Rannou, G., and Coddet, C., *Surf. Coat. Technol.,* 2002, vol. 157, p. 247.
13. Zhang, T., Huang, C., Lan, H., Du, L., and Zhang, W., *J. Therm. Spray Technol.,* 2016, vol. 25, p. 12.
14. Uyulgan, B., Dokumaci, E., Celik, E., Kayatekin, I., Ak Azem, N.F., Ozdemir, I., and Torpali, M., *J. Mater. Process. Technol.,* 2007, vol. 190, p. 204.
15. Redjdal, O., Zaid, B., Tabti, M.S., Henda, K., and Lacaze, P.C., *J. Mater. Process. Technol.,* 2013, vol. 213, p. 779.
16. Zabihi, A. and Soltani, R., *Surf. Coat. Technol.,* 2018, vol. 349, p. 707.
17. Liu, Y.-C., Lin, G.S., Wang, J.-Y., Cheng, C.-S., Yang, Y.-C., Lee, B.-S., and Tung, K.-L., S*urf. Coat. Technol.,* 2018, vol. 349, p. 357.
18. Komatsu, K., Costa, T., Ikeda, Y., Abe, K., Dan, Y.X., Kimura, T., Shirai, T., Nakamura, A., and Saitoh, H., *Int. J. Appl. Ceram. Technol.,* 2018, vol. 16, p. 254.
19. Barabás, R., Bogya, E.S., Dejeu, V.R., Bizo, L., Aneziris, C.G., Kratschmer, T., and Schmutz, P., *Int. J. Appl. Ceram. Technol.,* 2011, vol. 8, p. 566.
20. Davis, J.R., *Handbook of Thermal Spray Technology, Introduction to Thermal Spray Processing*, Materials Park, OH, ASM Int., 2004.
21. Babakhani, A., Zahabi, E., and Mehrabani, H.Y., *J. Alloys Compd.,* 2012, vol. 514, p. 20.
22. Luo, X.-X., Yao, Z.-J., Zhang, P.-Z., Miao, Q., Liang, W.-P., Wei, D.-B., and Chen, Y., *Appl. Surf. Sci.,* 2014, vol. 305, p. 259.
23. Li, Z.-F., Cao, G.-M., He, Y.-Q., Liu, Z.-Y., and Wang, G.-D., *Steel Res. Int.,* 2016, vol. 87, p. 1469.
24. Kim, M.J. and Lee, D.B., *Adv. Technol. Innovation,* 2017, vol. 2, p. 126.
25. Bose, S., *High Temperature Coatings*, Oxford: Butterworth-Heinemann, Elsevier, 2007.

26. Quanli, J., Haijun, Z., Suping, L., and Xiaolin, J., *Ceram. Int.,* 2007, vol. 33, p. 309.

27. Kurlov, A.S. and Gusev, A.I., *Inorg. Mater.,* 2011, vol. 47, p. 133.

28. Frutos, E., Adeva, P., Carrasco, J.L.G., and Pérez, P., *Surf. Coat. Technol.,* 2013, vol. 236, p. 188.

29. Horita, T., Yamaji, K., Xiong, Y., Kishimoto, H., Sakai, N., and Yokokawa, H., *Solid State Ionics,* 2004, vol. 175, p. 157.

30. Salgado, M.de F., Sabioni, A.C.S., Huntz, A.-M., and Rossi, É.H., *Mater. Res.,* 2008, vol. 11, p. 227.

31. Cheng, X., Jiang, Z., Monaghan, B.J., Wei, D., Longbottom, R.J., Zhao, J., Peng, J., Luo, M., Ma, L., Luo, S., and Jiang, L., *Corros. Sci.,* 2016, vol. 108, p. 11.

32. Zhang, N.-Q., Zhu, Z.-L., Xu, H., Mao, X.-P, and Li, J., *Corros. Sci.,* 2016, vol. 103, p. 124.

33. Lussana, D., Baldissin, D., Massazza, M., and Baricco, M., *Oxid. Met.,* 2014, vol. 81, p. 515.

34. Pérez, F.J., Cristóbal, M.J., and Hierro, M.P., *Oxid. Met.,* 2001, vol. 55, p. 165.

35. Grzesik, Z., Smoła, G., Adamaszek, K., Jurasz, Z., and Mrowec, S., *Oxid. Met.,* 2013, vol. 80, p. 147.